

Effects of the Building Block on the Morphology and Properties of Porous CdSe Nanostructured Framework

Hongtao Yu*, Robert Bellair**, Rangaramanujam M. Kannan** and Stephanie L. Brock*

*Department of Chemistry and **Department of Chemical Engineering and Material Science, Wayne State University, Detroit, USA, sbrock@chem.wayne.edu

ABSTRACT

A major challenge in designing and making potentially valuable nanostructures is to find suitable ways to effectively tune their properties and function. Recent work in our lab has demonstrated a powerful strategy to engineer the morphology and properties of metal chalcogenide 3-D nanostructured assemblies prepared by sol-gel methods. Here we show that by altering the shape of CdSe building blocks from dot to rod, the morphology of the gel can be altered from colloidal to polymeric. Notably, the polymeric (rod) aerogel has twice the surface area of the colloidal (dot) aerogel. Rheological studies of aerogel-PDMS (polydimethylsiloxane) composites indicate that the rod aerogel structure is stronger than the dot aerogel, and the reinforcement is due to the structure of the gel, not the particle geometry. Finally, in addition to dots and rods, the morphological consequences of CdSe branched and hyperbranched nanoparticles on resultant aerogels will also be discussed.

Keywords: CdSe nanodots, CdSe nanorods, morphology, gel strength

INTRODUCTION

Quantum dots (semiconducting nanoparticles) as a novel class of materials, have the potential to reform many current technologies and accordingly have received a great deal of attention from materials scientists. In the past several years, the research priority on semiconducting nanoparticles has changed from studies of size and shape dependent electronic and optical properties to designing more complex nanostructures^{1,2} and organizing simple nanometer scale building blocks into functional architectures.^{3,4} Recently, a general methodology has been developed in our lab to assemble quantum dots into 3-D porous networks without the presence of intervening surface ligands that can moderate dot-dot interactions.⁵ Experimental data suggest that the resultant architectures maintain the crystalline phase and quantum confinement of the building blocks and exhibit a colloidal morphology similar to that of a base-catalyzed silica aerogel.⁶ While the quantum dot aerogels exhibit relatively high surface areas, the structures are fragile and their surface areas are considerably lower than traditional silica aerogels. In order to alter and enhance the inherent properties of the metal

chalcogenide aerogel framework, including the morphology, gel strength, surface area and porosity, here we employed a new strategy to engineer these radical properties in semiconducting metal chalcogenide aerogels by changing the shape of the building block.⁷

Among the quantum dot systems, CdSe materials have been extensively studied by the scientific community due to the ability to precisely control the size and shape of CdSe nanoparticles and the fact that the optical properties of the particles can be tuned throughout the visible spectrum by varying the size and shape.^{8,9} There are two major shapes associated with CdSe nanoparticles: dot and rod. The rod shape demonstrates an anisotropic geometry and is expected to be a more rigid building block, compared with an isotropic dot. On the other hand, compared with an identical-diameter dot, the rod is less quantum-confined. Recent research suggests that the surface free energy of the apexes of CdSe nanorods are more chemically reactive than the facets along the axis due to the presence of more dangling bonds on the surface Cd atoms of the end facets.^{10,11} Indeed, it is this difference in reactivity that drives the formation of the nanorod in solution growth.¹² We postulate that when assembling rod-shaped CdSe nanoparticles into an aerogel network, this effect can significantly influence the way these nanorods interconnect and therefore lead to different inherent morphology, surface characteristics and porosity of resultant aerogels relative to analogs composed from spherical particles. We find that the CdSe aerogels assembled from rod-shaped building blocks exhibit a totally different morphology, much higher surface areas and better gel strength when compared with the corresponding dot aerogel.⁷

EXPERIMENTAL

CdSe dot nanoparticles. CdO powder (0.050 g, 0.37 mmole) was added to a mixture of TDPA (n-tetradecylphosphonic acid, 0.20 g, 0.72 mmole) and distilled TOPO (trioctylphosphine oxide, 4.0 g, 10.3 mmole), heated at 150 °C and kept under Ar flow for 30 min to remove residual water. Then the temperature was set to 320 °C and the brownish mixture was left under Ar flow for 6-7 hours, resulting in a colorless solution. The temperature was reduced to 150 °C. A solution containing 0.032 g selenium (0.30 mmole) in 2.5 mL TOP was rapidly injected at 150 °C. The temperature was then raised at a rate of 10 °C per 10 min up to 230 °C, and the solution was kept at this temperature for 4 hours before cooling down to 80 °C. 4 mL of toluene was injected and the particles

precipitated with an excess of ethyl alcohol. To purify the particles, the solution was centrifuged and the sediment was re-dispersed in toluene. After a second precipitation with ethyl alcohol, the sediment was kept for further analysis.

CdSe rod nanoparticles. CdO powder (0.15 g, 1.1 mmole) was added to a mixture of TDPA (0.70 g, 2.5 mmole) and distilled TOPO (4.0 g, 10.3 mmole), heated at 150 °C and kept under Ar flow for 30 min to remove residual water. Then the temperature was set to 320 °C and the brownish mixture was left under Ar flow for 4 hours. This step resulted in a colorless solution. The temperature was then reduced to 270 °C. A solution of 0.095 g selenium (1.1 mmole) in 1.5 mL TOP was rapidly injected at 270 °C. Then the temperature was decreased to 230 °C, and kept for 3 hours before cooling to 80 °C. Isolation and purification were conducted as described for dot-shaped CdSe nanoparticles.

MUA capping of CdSe nanoparticles, gelation and aerogel formation. For dot and rod-shaped CdSe nanoparticles, the 11-mercaptoundecanoic acid (MUA) solution was prepared by dissolving 0.8 g MUA (3.3 mmole) in 10 mL methanol solution with tetramethylammonium hydroxide pentahydrate (TMAH) added to achieve a system pH of 10.5-11. The solid precipitate of CdSe nanoparticles was then dispersed in the MUA solution and left stirring in a static Ar environment at 30 °C overnight. At room temperature, an excess amount of ethyl acetate was added to precipitate MUA-capped nanoparticles. The solution was centrifuged and the sediment was re-dispersed in methanol. After a second precipitation with ethyl acetate, the sediment was dispersed in 10 mL methanol for gelation.

Gelation was achieved by adding 10 µL of 3% tetranitromethane (TNM) to 2 mL aliquots of CdSe sols. The mixture was shaken vigorously and subsequently allowed to sit undisturbed for gelation. The resulting wet gels were aged for 7 days under ambient conditions. Aged gels were exchanged with acetone 6-7 times over 3 days and then transferred to a SPI-DRY model critical point dryer where they were subsequently washed and immersed in liquid CO₂ over 6 hours. The CO₂ exchanged gels were dried under supercritical conditions by raising the drier temperature to 39 °C, maintaining that temperature for 30 min, followed by venting of CO₂ gas to obtain CdSe aerogel.

Composite preparation. CdSe/polydimethylsiloxane (PDMS) composites were prepared first by mixing 0.1 g of CdSe aerogel or nanoparticles to excess cyclohexane and sonicating the mixture for 2 minutes. Then a solution of 4.9 g of PDMS in cyclohexane was added into the mixture and stirred for 24 hours, followed by being frozen at -40 °C and drying under vacuum to remove all solvents.

X-ray Powder Diffraction. Powder X-ray diffraction (PXRD) analysis was employed to study the structure, phase and crystallinity of the nanoparticles and resultant aerogels. A Rigaku RU 200B X-ray diffractometer (40 kV, 150 mW, Cu-K α radiation) with rotating anode was used

for X-ray diffraction measurements. Powdered samples were deposited on a low background quartz (0001) holder coated with a thin layer of grease. X-ray diffraction patterns were identified by comparison to phases in the International Centre for Diffraction Data (ICDD) powder diffraction file (PDF) database (release 2000).

Transmission electron microscopy. Transmission electron microscopy (TEM) was employed to study the three CdSe different building blocks and the morphology of the resultant aerogels. The TEM analyses were conducted in the bright field mode using a JOEL FasTEM 2010 HR TEM analytical electron microscope operating at an accelerating voltage of 200 kV. Particle samples were prepared by depositing a drop of a dilute toluene dispersion of CdSe nanocrystals on carbon-coated copper grids and subsequently evaporating the solvent. Aerogel samples were prepared on carbon-coated copper grids by first grinding the aerogel to fine powders and then pressing the TEM grid onto the dried powder.

Surface area and porosimetry. The surface areas of CdSe aerogels were obtained by applying the BET model to nitrogen adsorption/desorption isotherms. A Micromeritics ASAP 2010 surface area analyzer was used to produce nitrogen physisorption isotherms at 77 K on powdered CdSe aerogel samples. The data were fit by using a Brunauer-Emmett-Teller (BET) model to determine the surface areas of the aerogels. The average pore diameter and cumulative pore volume were calculated by using the Barrett-Joyner-Halenda (BJH) model. Samples were degassed under vacuum at 100 °C for 48 hours prior to the analysis and employed a 30 s equilibrium interval and a 5 cc dose for a total running time of about 13 hours. Three independently prepared samples were analyzed for polymer-type aerogels prepared from rod building blocks, and compared with previously studied colloid type aerogels prepared from spherical building blocks.

Optical absorption and photoluminescence measurements. Optical absorption measurements of MUA capped CdSe nanoparticles in methanol were obtained on a Hewlett-Packard (HP) 8453 spectrophotometer. A dilute CdSe nanoparticle solution was analyzed against a methanol blank in the region from 400 nm to 700 nm. A Jasco V-570 UV/VIS/NIR spectrophotometer equipped with an integrating sphere was used to measure the optical diffuse reflectance of CdSe aerogels. Powdered aerogel samples were evenly spread on a sample holder pre-loaded with a reflectance standard and measured from 200 nm to 1500 nm. The band gaps of the samples were estimated from the onset of absorption in data converted from reflectance.

Emission properties of the CdSe nanoparticle precursors and corresponding aerogels were investigated using photoluminescence spectroscopy. A Cary Eclipse (Varian, Inc.) fluorescence spectrometer with 5 nm excitation and emission slits was used for photoluminescence studies. A dilute MUA-capped CdSe nanoparticle solution in methanol was placed in a 10 mm

quartz optical cell and analyses were done under ambient conditions. Powdered aerogel samples were sealed in evacuated quartz tubes and analyses were done at liquid nitrogen temperature. Monolithic aerogel samples were analyzed at room temperature.

RESULTS AND DISCUSSION

CdSe semiconducting nanoparticles were synthesized by typical high temperature colloidal methods to yield highly monodisperse CdSe nanodots and nanorods.⁸ These nanoparticles were then surface modified with thiolate ligands by treatment with 11-mercaptoundecanoic acid in the presence of tetramethylammonium hydroxide pentahydrate. Finally, controlled oxidative removal of the surface thiolate ligands led to gel formation, concomitant with the production of disulfide as a byproduct, and supercritical CO₂ drying yielded aerogel monoliths. TEM images in Figure 1 demonstrate the different building blocks and the morphology of the resultant aerogels. The CdSe rod aerogel exhibits a totally different morphology than the colloidal type dot aerogel and is similar to an acid-catalyzed silica aerogel with a polymer-type framework. This confirmed the hypothesis that altering the shape of the building block can be alternative way to change the morphology of resultant aerogels, instead of changing the gelation mechanism as is done with silica.¹³ The high resolution TEM images reveal the crystallinity of the building blocks for both types of aerogel (Figure 2). The lattice fringes can be attributed to hexagonal CdSe in all cases, confirmed by powder X-ray diffraction measurements on bulk samples. We postulate that the mechanism for the formation of the polymer morphology involves preferential connectivity of rods at the ends due to the higher surface free energies of the apical facets. This leads to a more penetrating aerogel framework than for the dots.

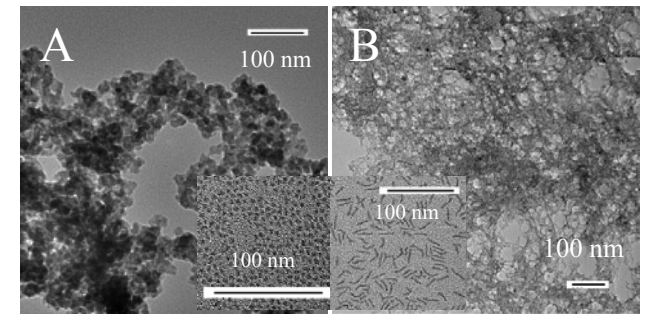


Figure 1: TEM images of A) CdSe dot aerogel, B) CdSe rod aerogel. Insets are different building blocks (dots and rods). The data were reproduced with permission from reference 7. Copyright 2008 American Chemical Society.

The surface area and porosity analyses were conducted with a Micromeritics model ASAP 2010 surface area analyzer using nitrogen physisorption isotherms performed at 77 K on powder aerogel samples. The data in Table 1

show that the CdSe rod aerogels exhibit double the surface area value of the dot aerogels based on the BET model, and over twice the cumulative pore volume using BJH model (based on cylinder pore). This strongly proves that altering the building blocks is an effective way to engineering the critical parameters of quantum dot aerogels. More interestingly, in silica aerogels, the polymer-type aerogel (acid-catalyzed) exhibits lower surface areas than the colloid-type aerogel (base-catalyzed);¹⁴ conversely in CdSe aerogels, the polymer-type rod aerogel shows a much higher surface areas than colloid-type dot aerogel.

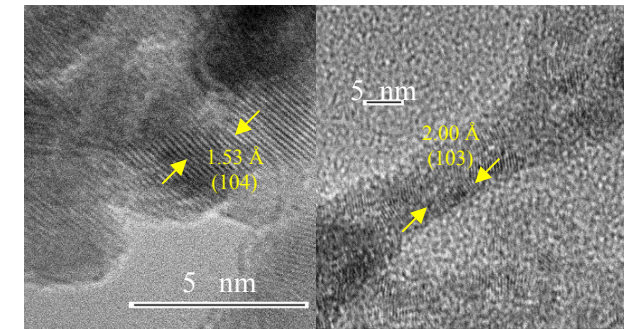


Figure 2: High resolution TEM images of CdSe dot (left) and rod aerogels (right). The data were reproduced with permission from reference 7. Copyright 2008 American Chemical Society.

Table 1: Brunauer-Emmett-Teller (BET) surface areas, Barrett-Joyner-Halenda (BJH) absorption average pore diameters and BJH cumulative pore volumes of CdSe colloidal and polymeric aerogels (average of three independent samples); primary particle size and optical bandgap of the building block and aerogel. The data were reproduced with permission from reference 7. Copyright 2008 American Chemical Society.

CdSe aerogel	colloidal	polymeric
BET surface area (m ² /g)	107 ± 10	239 ± 7
average pore diameter (nm)	35.4 ± 2.4	24.5 ± 1.5
Cumulative pore volume (cm ³ /g)	0.59 ± 0.31	1.64 ± 0.11
size of building block (nm)	3.17 ± 0.31 (dot)	3.4 ± 0.33 × 22.7 ± 2.2 (rod)
Absorption onset value Primary particle / aerogel (eV)	2.15 / 2.12	2.06 / 2.02

The band gap and emission measurements reveal that both types of CdSe aerogel maintain a nearly identical degree of quantum confinement as seen in the respective building blocks from which they were assembled. This is manifested in a nearly identical band gap value (Table 1)

and emission peak energy as is observed in the particle components. More impressively, the CdSe rod aerogel monolith shows much stronger band edge emission peak than the dot aerogel monolith with the same mass and under the identical experimental conditions (Figure 3). The emission intensity ratio for the maxima between the rod monolith and dot monolith is 25:1.

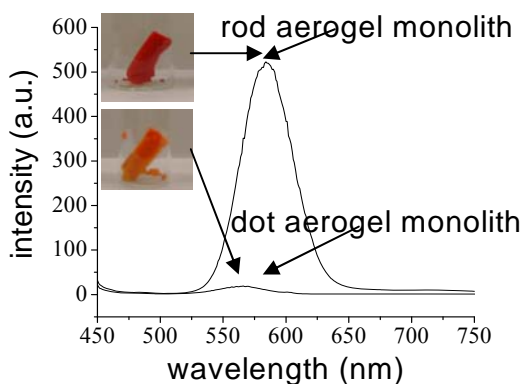


Figure 3: Graph of room temperature emission spectra ($\lambda_{\text{ex}} = 440 \text{ nm}$) of CdSe dot and rod aerogel monoliths (pictured in insets) with the same mass (dot: 0.0183g/ rod: 0.0181g). The data were reproduced with permission from reference 7. Copyright 2008 American Chemical Society.

Another distinct difference between the CdSe dot gel and rod gel is that the rod gel exhibits a much smaller tendency to shrinkage of the gel body-i.e., the syneresis effect in which a wet gel expels solvent is less pronounced in the rod gel relative to the dot gel. Thus rod gels can be inverted in contrast to dot gels (Figure 4 inset). This phenomenon indicates that the CdSe polymer-type rod aerogel might be much stronger than colloid-type dot aerogel. To quantify this gel strength property, rheological studies were conducted on aerogel-PDMS (polydimethylsiloxane) composites for a weight percentage of 5% CdSe. Rheology data show that rod aerogel-PDMS composites exhibit a much higher complex viscosity than dot aerogel-PDMS composites and rod aerogels result in an enhanced system modulus over the dot aerogel. (Figure 4) This enhancement is not due to the identity of the building block, since composites formed from dot and rod primary particles show identical (and considerably lower) viscosities relative to the aerogels. This strongly suggests that the enhanced strength is a consequence of the morphology of the interconnected networks.

Altering the building block appears to be an effective way to engineer the basic properties of metal chalcogenide semiconducting aerogels. This novel strategy might offer a powerful manner to tune specific properties of the nanostructure for targeted applications. In addition to the comparison between CdSe dot and rod aerogels, the effects of other shapes, including CdSe branched and hyperbranched nanoparticles, on the morphology and properties of resultant aerogels will be also discussed.

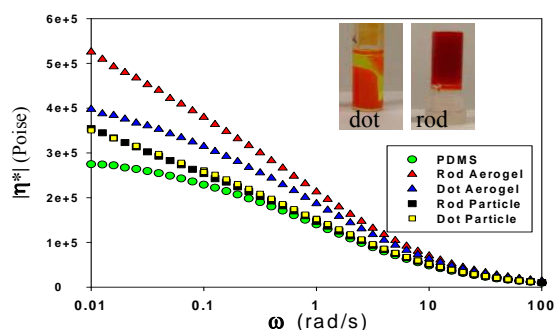


Figure 4: Complex viscosity data for PDMS and PDMS composites of dots, rods, and corresponding aerogels (5 wt. % CdSe). The insets show the effect of syneresis on shrinkage of dot gels relative to rod gels. The data were reproduced with permission from reference 7. Copyright 2008 American Chemical Society.

ACKNOWLEDGEMENT

We thank Dr. Yi Liu for assistance with TEM measurements. This work was supported in part by the Donors of the Petroleum Research Fund (AC-43550), NSF (DMR-0701161, DMR-0216084), and the Institute of Manufacturing Research (WSU).

REFERENCES

- [1] D. J. Milliron, S. M. Hughes, Y. Cui, L. Manna, J. Li, L.-W. Wang and P. A. Alivisatos, *Nature*, 430, 190-195, 2004.
- [2] R. D. Robinson and P. A. Alivisatos, *Science*, 317, 355-358, 2007.
- [3] Z. Tang, Z. Zhang, Y. Wang, S. C. Glotzer and N. A. Kotov, *Science*, 314, 274-278, 2006.
- [4] E. V. Shevchenko, D. V. Talapin, N.A. Kotov, S. O'Brien and C. B. Murray, *Nature*, 439, 55-59, 2006.
- [5] J. L. Mohanan, I. U. Arachchige and S. L. Brock, *Science*, 307, 397-400, 2005.
- [6] I. U. Arachchige and S. L. Brock, *J. Am. Chem. Soc.*, 128, 7964-7971, 2006.
- [7] H. Yu, R. Bellair, R. M. Kannan and S. L. Brock, *J. Am. Chem. Soc.*, 10.1021/ja801212e, 2008.
- [8] Z. A. Peng and X. Peng, *J. Am. Chem. Soc.*, 123, 183-184, 2001.
- [9] X. Peng, *Adv. Mater.* 15, 459-463, 2003.
- [10] T. Mokari, E. Rothenberg, I. Popov, R. Costi and U. Banin, *Science*, 304, 1787-1790, 2004.
- [11] J. E. Halpert, V. J. Porter, J. P. Zimmer and M. G. Bawendi, *J. Am. Chem. Soc.*, 128, 12590-12591, 2006.
- [12] Z. A. Peng and X. Peng, *J. Am. Chem. Soc.*, 123, 1389-1395, 2001.
- [13] N. Hüsing and U. Schubert, *Angew. Chem. Int. Ed.*, 37, 22-45, 1998.
- [14] M. L. Anderson, C. A. Morris, Stroud, R. M.; C. I. Merzbacher and D. R. Rolison, *Langmuir*, 15, 674-681, 1999.